

# Chapter 5

## Vibration Damping Systems with Shear Thickening Fluid



Mohammad Rauf Sheikhi, Selim Gürgen, and Melih Cemal Kuşhan

### 5.1 Introduction

Vibration is an undesired phenomenon due to the detrimental effects on structural stability, position control, materials performance, fatigue life, and noise reduction. This topic is of concern to a broad range of structures from automobiles to tall buildings. Vibration damping is a special field of interest to suppress the vibrations acting on the structures. Damping capacity and structural stiffness are desired to be increased in vibration damping studies [1].

Vibration damping systems use passive or active solutions to suppress the vibrational loadings on the structures. In passive solutions, materials with high damping characteristics are included into the structures. These materials provide an enhanced absorption capability to the vibrational energy acting on the structures. For example, vibrational energy can be transferred into mechanical deformation or heat loss on the damping materials, thereby providing passive vibration attenuation for the structures. On the other hand, active systems require an external power for the sensors and actuators that are used to counter the vibrations on the structures [1]. As a major advantage of active systems over passive ones, resonances can be avoided by tuning the damping systems, thereby preventing from structural collapses at natural frequencies.

---

M. R. Sheikhi

Key Laboratory of Traffic Safety on Track of Ministry of Education, School of Traffic & Transportation Engineering, Central South University, Changsha, Hunan, China

State Key Laboratory for Strength and Vibration of Mechanical Structures, Shaanxi ERC of NDT and Structural Integrity Evaluation, School of Aerospace Engineering, Xi'an Jiaotong University, Xi'an, China

S. Gürgen (✉) · M. C. Kuşhan

Department of Aeronautical Engineering, Eskişehir Osmangazi University, Eskişehir, Turkey  
e-mail: [sgurgen@ogu.edu.tr](mailto:sgurgen@ogu.edu.tr)

Various materials are used in passive vibration damping systems. In general, viscoelastic properties are demanded from the materials. Polymers and rubbers are widely used for this purpose [2]. Vibrational energy is attenuated through heat loss by the effect of viscoelastic characteristics of the materials. In addition to viscoelasticity, microstructural defects in metal alloys such as dislocations, grain boundaries, and secondary phases are benefitted in vibration damping systems. In metal-based vibration damping systems, vibrational energy triggers the activation of defects such as slip motions and plastic deformations in metal alloys and consequently leading to vibration damping through energy conversion in the structures [3].

Due to its unique rheological behavior, shear thickening fluid (STF) has been adapted to different vibration damping systems in recent years. STF has low viscosity properties under rest or low frequency conditions; however, its viscosity significantly increases upper levels upon exciting by high-frequency loading. STF exhibits excellent viscous damping behavior as well as good elastic stiffness capabilities, and for this reason, it emerges as a passive dissipative material suitable for vibration damping systems [4–6]. Unlike active damping devices, STF does not require an additional power unit for activation because its rheological response naturally activates in case of an external stimulation [7, 8]. Tailoring the rheological response for the desired damping properties provides excellent advantages for the users, thereby eliminating the complexity as such in the fluid-based active damping systems requiring magnetic or electric fields.

Vibration control is an essential issue for many fields. However, three main application areas come to the forefront considering the STF-based vibration damping systems in the literature: structural components, machinery, and manufacturing. In this chapter, STF-based vibration damping systems are discussed for the given application areas.

## 5.2 STF-Based Vibration Damping in Structural Components

In order to enhance the vibration damping properties of structures, STF is generally merged into conventional components instead of using it as a single body because STF is a fluidic material. For this reason, holes and channels are typically designed in structural components to be filled with STF. Gürgen et al. [9] designed sandwich panels having an extruded polystyrene (XPS) core material between aluminum face sheets. A set of holes was drilled in the core material to contain STF. Modal analysis method was employed to find out the damping ratios in the sandwich structures. In this simple technique, structures are excited by hammer impacts to show their natural vibrations. An accelerometer is used to collect the free vibrations in terms of displacement, and then mass, damping, and stiffness metrics are calculated for overall system. Complex systems such as STF-included structures show multi-degree of freedom, which is transformed into a set of single-degree of freedom systems by

this way. Consequently, complex problems can be modeled as linear superposition of a number of single-degree of freedom systems in modal analysis. According to this work, STF integration into the sandwich structures leads to a significant increase in the damping ratios. Based on an early study [10], liquid addition into the structures contributes to the damping properties regardless of liquid rheology. Because the liquid acts as a viscous medium in the system and thereby provides a damping mechanism for the structures. Liquid sloshing lowers the vibrations acting on the structures [11]. Despite the conventional viscous effect in any liquid, STF provides an additional damping mechanism for the structures. When the STF-containing sandwich panels are excited by vibrational loading, STF in the holes starts flowing and particle interactions are observed in the microstructure. By the effect of vibrational stimulation, hydrodynamic interactions grow up in the flow field and, consequently, particles are forced to get close to each other. Particle contacts, which support the shear thickening effect, may be observed depending on the loading level. As particle contacts predominate the microstructure, shear thickening effect grows stronger. For this reason, STF shows stiffer characteristics under vibrational loading, thereby contributing to the damping properties of the structures [9].

Fischer et al. [12] investigated the vibration control properties of multi-layer composites intercalated with STF. The aim of this work was understanding the effect of STF inclusion on the stiffness and damping capacity of the composite under dynamic deformation. In line with this purpose, a layer of STF was spread between polyvinyl chloride (PVC) beams. The STF was fabricated by distributing hydrophilic fumed silica in a polypropylene glycol (PPG) pool. In the vibrating beam testing, one of the beam ends was fixed by a clamp while the other end was exposed to forced oscillations by a vibration generator. A laser velocity transducer was used for monitoring the displacement at the tip of the excited beam end. The amplitude of the stimulation was adjusted instantly to keep the displacement amplitude constant. A data recording unit was used to track the corresponding forces with respect to frequency for different levels of displacement amplitudes. From the experimental results, the relative motion of the PVC beam is heavily affected by the shear thickening rheology. Above a certain amplitude, which corresponds to the thickening point of STF, the natural frequency of the beam increases while growing the vibration damping performance in the multi-layer structure.

A similar beam design was proposed by Wei et al. [13]. Aluminum face sheets with an STF core layer were considered in this work. The dynamic characteristics were theoretically investigated by considering an external forced excitation. STF properties were taken into account while the governing equation for the beam was derived from the complex stiffness method and Timoshenko beam theory. In the calculations, the following were assumed: (1) the Euler-Bernoulli beam theory is valid for face sheet deformations, (2) low mode vibration is considered for the beam, (3) only shear deformations act in STF core, (4) all the layers (face sheets and STF core) show identical transverse displacements, and (5) no slip and delamination conditions for the interfaces during deformation. Various parameters were selected to understand their effects on the dynamic properties of the structure. These parameters were excitation frequency, excitation amplitude, excitation location, and

skin/core thickness ratio. According to the results, natural frequency is quite dynamic by integrating STF core into the beam unlike traditional structures. Moreover, natural frequency gets more sensitive at higher excitation amplitudes. In addition, the sensitivity of the natural frequency is prone to increase at lower excitation frequencies. On the other hand, the variation in the natural frequency gets bigger when the excitation location is near the mid-span of the structure. There is a certain relationship between the skin/core thickness ratio and natural frequency. When the skin/core thickness ratio increases, the natural frequency increases as well. To sum up, STF inclusion in the aluminum-based beams leads to a reduction in the vibration of the structures [14]. The non-Newtonian rheology of STF provides a thickened texture in the core of the beam under loading. From this change, stiffness and damping characteristics in the structures are enhanced and, consequently, vibration attenuation behavior is enhanced.

In another study, STF was incorporated into carbon fiber reinforced polymers (CFRP) tubes [15]. Although CFRP-based components are widely used in aerospace, automotive, sport, and medical equipment applications, this material needs an improvement in the vibration damping properties. The STF was made from natural products such as cornstarch and water. Three different cornstarch loadings (50%, 55%, and 60%) were used in the STF fabrication. After filling the CFRP tubes with STF, the specimens were tested in modal analysis. Two different clamping configurations were selected in the experimental setup as shown in Fig. 5.1. According to the results, the tubes without STF exhibit the lowest damping ratio while damping ratio increases by filling the tubes with higher cornstarch content mixtures. These results indicate that STF addition leads to a gain of performance for damping behavior. Moreover, vibration damping performance simply depends on the shear thickening effect. To understand the role of shear thickening effect, thickening ratio was calculated for all suspensions having different cornstarch amounts. Thickening ratio is a performance metric for the better understanding of shear thickening intensity in

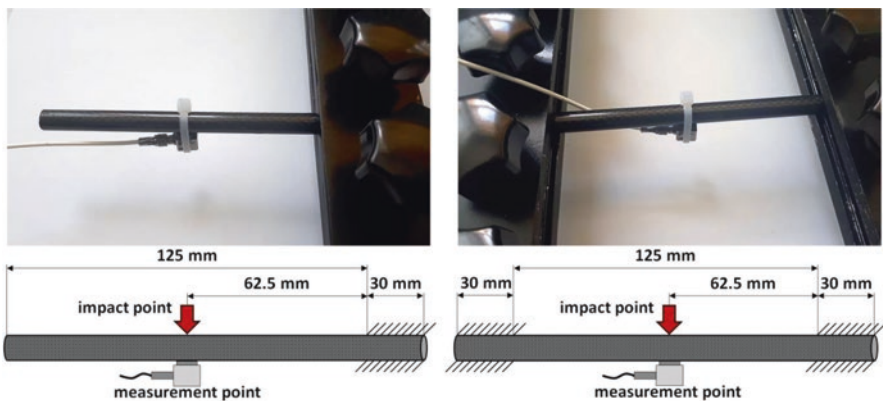


**Fig. 5.1** Vibration test setup for single-fix end and double-fix end [15]. Reprinted by permission from Elsevier

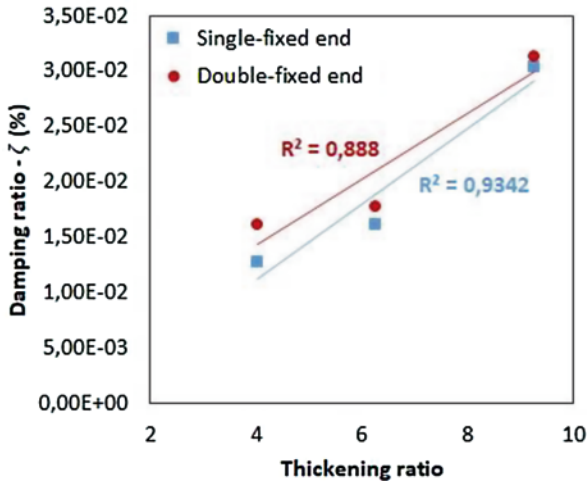


Fig. 5.2 Damping ratio vs thickening ratio [15]. Reprinted by permission from Elsevier

the suspensions. This metric is defined as the peak viscosity beyond the thickening point over the viscosity at the critical shear rate [16]. Figure 5.2 shows the correlation between the damping ratio of the tubes and the thickening ratio of the STFs. It is clearly seen in the chart that shear thickening intensity has a direct relationship with the vibration damping behavior of the structures. As the solid particle loading increases in the suspension, thickening ratio increases and, therefore, peak viscosity at the thickening regime reaches upper levels. Consequently, STF-included tubes behave in stiffer manner and damping properties get stronger by this means. The novel STF/CFRP design is suggested for unmanned aerial vehicle (UAV) structures to enhance the vibration isolation properties against flutter and undesired vibrations during flights.

The thickening ratio level regarding the particle loading aforementioned in the previous paragraph can be associated with the clustering mechanism in the suspension. In denser mixtures, clustering mechanism quickly takes place due to the increased hydrodynamic interactions. For this reason, lower critical shear rates are frequently encountered in the rheological measurements, which means that the onset of the thickening phenomenon can be easily observed at lower rate of external stimulations. In other words, thickening threshold in terms of shear forces can be reached at lower shear rates by adding more solid particles in the mixtures. This is due to the decreasing inter-particle distances, which enhance the particle interactions as well as overcoming the repulsive forces between the particles [17]. In addition to the hydrodynamic effect, dense suspensions are more prone to produce particle contacts in their microstructures especially at higher shear rates. Because small inter-particle distances lead to strong attraction forces between the particles and consequently physical contacts inevitably take place in the microstructures. From this formation, shear thickening effect gets stronger in the mixtures, thereby increasing stress transfer both in the suspension and at the STF/CFRP interfaces. As

a result of this process, vibration damping characteristics are enhanced in the STF-included structures [15].

The key point in benefiting from STF in vibration damping is tailoring the thickening phase to coincide with the structural resonance point. At the shear thickening regime, the suspension shows increased stiffness and thereby provides strong damping behavior at that state. Regarding this important issue, Neagu et al. [18] proposed a micromechanical approach to STF-integrated composite structures. In this work, a block of silicone was reinforced by a set of glass fiber/epoxy rods. The interfaces between the silicone matrix and reinforcing rods were nested for an STF made from spherical silica particles and polyethylene glycol (PEG). The composites were subjected to dynamic mechanical analyses to determine the dynamic properties. According to the experimental results, STF presence at the matrix/reinforcement interfaces significantly enhances the damping behavior of the composites. The dynamic properties are heavily dependent on frequency and applied external load amplitude. Damping peaks are observed at the shear thickening regime of the STF, which clearly proves that shear thickening provides an additional damping capability for the structures. In addition, the damping peak locations appear depending on the onset of shear thickening rheology in the STF. In this sense, STF-integrated composites are capable of stiffness/damping control for certain vibration frequencies. To do this, STF rheology can be tailored in many different ways. STF rheology depends on several factors, which can be manipulated for tuning the shear thickening behavior. Particle volume fraction, particle aspect ratio, particle size, particle roughness, particle modifications, liquid medium, temperature, and reinforcing fillers are the main factors providing an opportunity for rheological control [16, 19–21].

### 5.3 STF-Based Vibration Damping in Machinery

STF-based vibration control in machinery has been an interesting topic for two decades. A damper is a simple solution in conventional applications. From this point of view, researchers have made great efforts to integrate STF into a simple device and ultimately propose a passive adaptive damper for machinery applications. The first attempt about including STF in traditional dampers is replacing the hydraulic oil with STF. The viscoelastic damping characteristics of the dampers gain an adaptive behavior by this way.

Zhao et al. [22] proposed an STF-based damper for adaptive vibration attenuation in rotary systems. The STF was synthesized by distributing nano-size fumed silica in PEG medium. Then this smart suspension was filled in a damper, which was investigated in a rotary test setup as shown in Fig. 5.3. In the experimental stage, two STF dampers were attached to a rotor system in x and y directions to suppress the undesired vibrations generated by the rotary motion. Vibration frequencies and vibration amplitudes were investigated in this experimental work. Figure 5.4 shows the dynamic response of the rotary system. As shown in Fig. 5.4a and b, there are quite large displacements in the no-damper cases. By attaching one



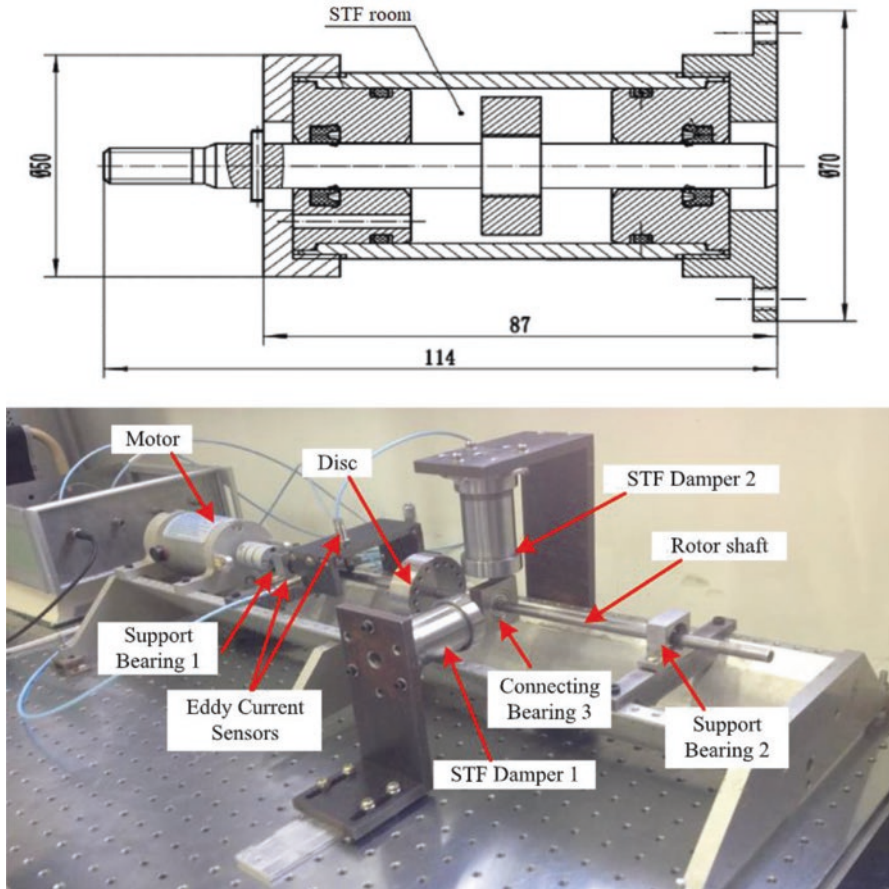


**Fig. 5.3** Structural design of STF damper and vibration test setup [22]. Reprinted by permission from Elsevier

STF damper whether in x or y directions, the displacements are effectively restricted to a small area. Moreover, the displacements show higher restrictions in the STF damper installation directions. On the other hand, the displacements are significantly reduced and, thus, the stability of the rotary system is highly enhanced by using two STF dampers in both directions. From the chart given in Fig. 5.4c, it is possible to state that the first-order resonance amplitude of the rotary system is about 90  $\mu\text{m}$  in x-direction for the no STF damper case. The resonance amplitude greatly reduces to about 15  $\mu\text{m}$  and 40  $\mu\text{m}$  by using an STF damper in x-direction and y-direction respectively. On the other hand, a significant reduction is obtained in the two STF damper case that the resonance amplitude shows only 4  $\mu\text{m}$  by the effect of STF damping in both directions. Similar improvements are achieved in the resonance amplitudes in y-direction as shown in Fig. 5.4d. As given in the graph, the resonance amplitude of the system without a damper is about 400  $\mu\text{m}$ , whereas it is

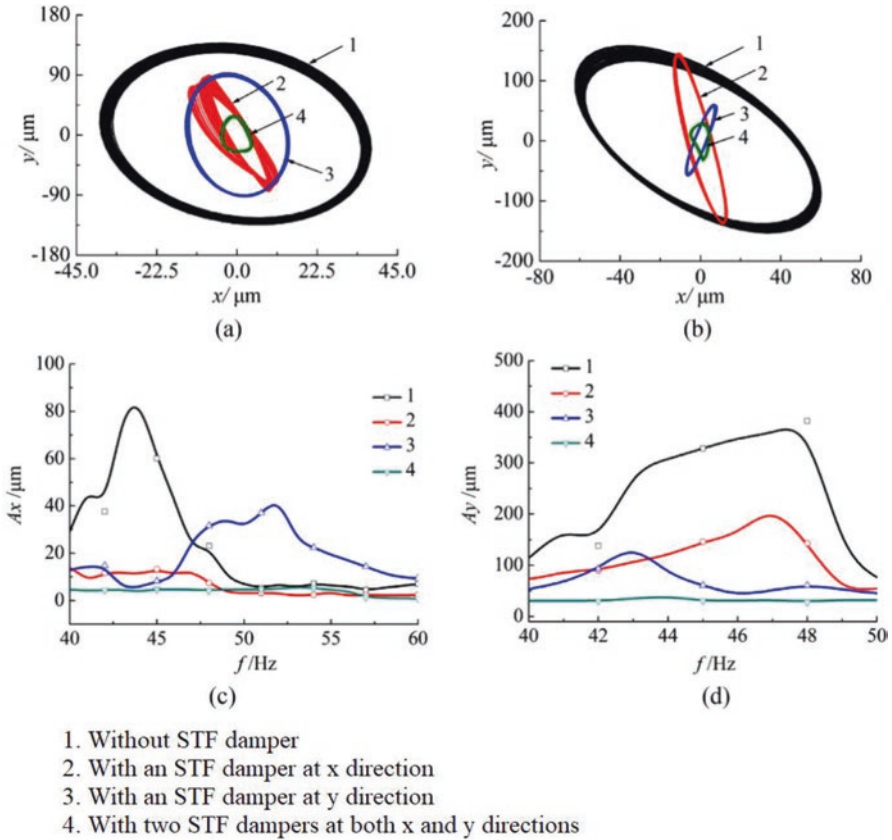


**Fig. 5.4** Dynamic response of the rotary system: (a) axis orbits with a frequency of 42 Hz, (b) axis orbits with a frequency of 45 Hz, (c) x-direction amplitude response nearby resonance region, and (d) y-direction amplitude response nearby resonance region [22]. Reprinted by permission from Elsevier

about 220  $\mu\text{m}$  and 140  $\mu\text{m}$  for the one STF dampers attached in x-direction and y-direction, respectively. The highest suppression is achieved in the two STF damper case, which yields a resonance amplitude of about 30  $\mu\text{m}$ . There is an obvious improvement in the vibration attenuation properties by using STF dampers in the rotary mechanism.

STF dampers have nonlinear characteristics due to the rate-dependent behavior of STF rheology and show large damping forces. For this reason, they provide enhanced energy absorption capabilities at natural frequencies in comparison to the conventional linear dampers. Furthermore, damping force in STF dampers can be increased significantly depending on the frequency and amplitude and, therefore, stronger vibration suppression properties are clearly obtained in these smart devices. Unbalanced vibrations in rotary systems especially at natural frequencies can be effectively attenuated by the nonlinear damping characteristics. STF dampers have



a great potential to be integrated into adaptive or semi-active vibration control systems [22].

In another STF damper study, Wei et al. [23] developed a phenomenological model for predicting the flow characteristics of STF. Then, an analytical model was proposed to simulate the dynamic characteristics of an STF damper by the aid of the developed phenomenological model for STF rheology. In the damper modeling, force-displacement curves were investigated for various amplitudes and frequencies. According to the results, peak damping forces greatly increase as the amplitudes and frequencies increase in the system. Contrary to the magnetorheological dampers, force-displacement curves in STF dampers do not follow stable characteristics under increasing excitations. At significantly large amplitudes and frequencies, damping forces are prone to get lower values beyond a critical point. Furthermore, the reduction in damping forces becomes prominent by decreasing the annular gap. For this reason, annular gap dimension is one of the key factors in STF damper design, especially for large amplitude and frequency applications.

Lin et al. [24] designed a damper filled with fumed silica and PEG-based STF. The damper was subjected to sinusoidal loadings while imposing different frequencies. The dynamic behavior of this smart damper was investigated by considering the force-displacement and force-velocity curves. From the results, damper forces exhibit a reduction by increasing the loading cycles for all frequencies. This effect grows upon long-term loadings. The root cause is found as the heat generation in the damper system and consequently increasing temperature. Based on the previous works [25–29], shear thickening behavior shows a degradation at elevated temperatures due to lower rate of hydrodynamic interactions. For this reason, a gradual reduction in peak viscosity develops as the loading is applied to the damper. As a result, damping properties show a loss of performance for long-term operations. Although STF inclusion in damper systems provides an improvement for the dynamic properties, temperature has a restrictive effect on STF performance. From this point of view, an attempt is required to control the heat generation in STF-based damping devices.

Apart from conventional damper devices, STF was brought together with a sliding friction (SF) isolator to benefit from shear thickening rheology [30]. This device is suggested for anti-seismic applications to keep the structures in a stable position during cyclic loadings. The STF-based SF isolator includes a traditional SF material and STF as well. Figure 5.5 shows the details of STF-based SF isolator. At low excitation energies, the SF material protects the structure from large vibrations and displacements. On the other hand, STF provides a large damping forces by dissipating the external energy acting at high excitation cases. Consequently, the relative motion between the upper plate and the lower member is restricted to keep the structure static. For better understanding of the concept, a mechanistic approach was made by building an analytical model based on the flow momentum equations. The system was subjected to cyclic loadings with various accelerations. From the chart given in Fig. 5.6a, the upper plate shows excessive displacement with reference to the base member when the isolator is assembled without SF material and STF. On the other hand, almost no displacements are visible in the STF and SF/STF

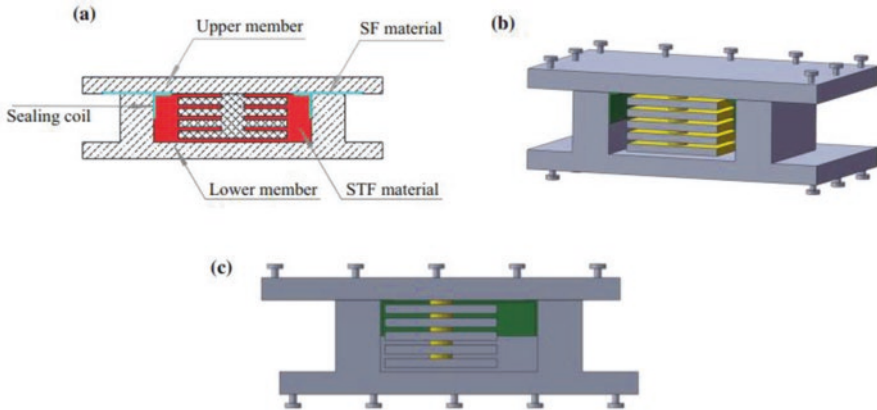


**Fig. 5.5** (a) Cross-sectional view of STF-based sliding friction isolator, (b) three-dimensional view of STF-based sliding friction isolator, and (c) STF-based sliding friction isolator after deformation [30]. Reprinted by permission from Springer Nature

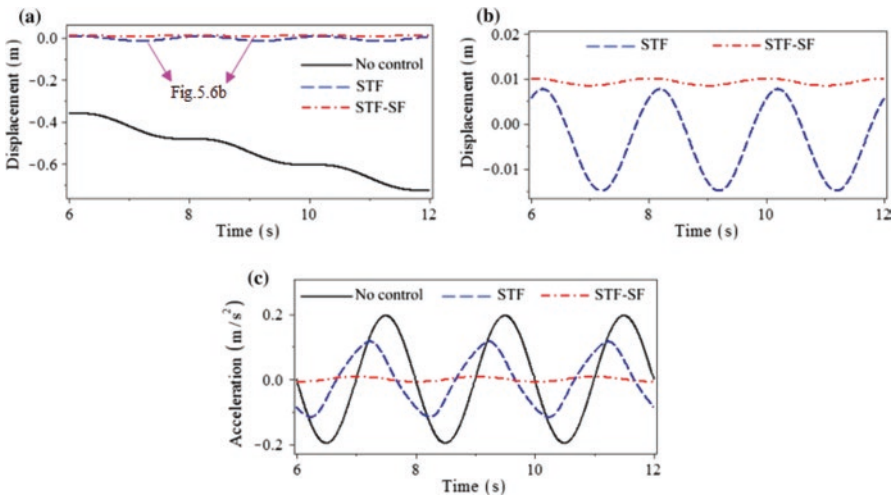


**Fig. 5.6** (a) General displacement response, (b) magnified displacement response, and (c) acceleration response of the isolators under a cyclic excitation acceleration of 0.01 g [30]. Reprinted by permission from Springer Nature

cases. Figure 5.6b shows a detailed view of the displacement curves in the STF and SF/STF cases. It is clearly seen that the average displacement for the SF/STF isolator is about 0.01 m while the amplitude is only 0.001 m. On the other hand, average displacement is about 0.005 m; however, larger amplitudes about 0.01 m are visible in the STF case. From these results, it is possible to mention that the SF/STF isolator provides more stable characteristics for vibration damping. The acceleration response of each system is given in Fig. 5.6c. The system without SF material and

STF exhibits large acceleration peaks during the cyclic loading. The accelerations are varied in a range of  $\pm 0.2 \text{ m/s}^2$ . In the STF case, the accelerations are suppressed to a range of  $\pm 0.1 \text{ m/s}^2$ . On the other side, the system with the SF/STF isolator shows almost no accelerations, which means that the system is quite stationary under the harmonic excitations. It can be stated that STF inclusion in the SF isolators provides a gain of performance for suppressing the excitations; however, SF sealing at the interface of the upper and lower members significantly enhances the damping characteristics. It can be mentioned that STF inclusion in the conventional SF isolators adds a value in terms of damping properties. Smart device concept is introduced with the SF isolators by integrating STF into these devices. Although the SF/STF isolator shows excellent properties, the design of the device can be enhanced for gain of performance. As an example of improvement, the layered design of columnar structure in the STF room can be optimized for increased shear thickening formation.

Another vibration damping device for machinery is damping pads. In the conventional applications, damping pads are generally made from elastomers to suppress the undesired vibrations through viscoelastic damping. Damping pads are easy-to-use and cost-effective solutions for anti-vibration applications. These pads are used as a support element in the installation of a wide range of large machines such as machining centers, sewing machines, belt lines, rotary mixers, and shakers. In recent applications, STF-based anti-vibration pads have been designed to take advantage of the adaptive damping behavior of STF in vibration isolation.

Cork is a potential material for anti-vibration systems due to its excellent damping behavior. There are many applications with the usage of cork in vibration isolation applications especially damping in machinery. One of them is incorporating STF into cork panels to gain smart damping pads for machinery applications. Gürgen et al. [31] designed multi-layer cork structures by applying STF as an adhesive between the layers. The STF used in this work was based on nano-size fumed silica and PEG. They constructed 20 mm thick cork pads with different numbers of layers as shown in Fig. 5.7. Vibration attenuation properties of these novel pads

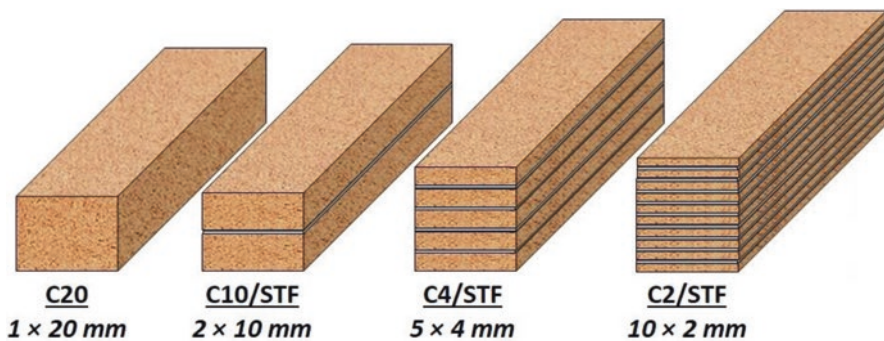
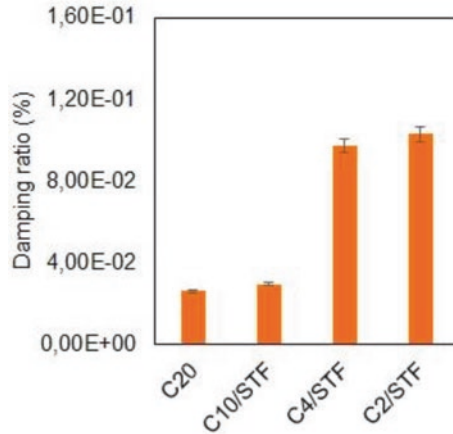


Fig. 5.7 STF-included cork pads for vibration isolation [31]. Reprinted by permission from Elsevier



**Fig. 5.8** Damping ratios for the multi-layer pads [31]. Reprinted by permission from Elsevier

were investigated by modal analysis considering the damping ratios. Figure 5.8 shows the damping ratios for the STF-included cork pads. From the results, there is a slight improvement in the damping behavior from the C20 to C10/STF pad. However, a clear jump in damping ratio is observed in the C4/STF and C2/STF pads. By using the STF at the cork layer interfaces, vibration suppression is enhanced and, furthermore, this effect is pronounced by increasing the number of STF intercalated layers in the pads. This is simply related to the STF amount increasing with the increased number of interfaces. For example, the C10/STF pad includes only 1 g of STF, whereas it is 9 g in the C2/STF pad. Replacing the C10/STF pad with the C2/STF one in a machinery application, shear thickening formation takes place in an increased number of layers within the structure. As a result of this, structural stiffness grows stronger in the C2/STF pad. From the microstructural aspect, silica particles introduce with hydrodynamic loading upon vibrational excitation. The particles are restricted in clusters within the liquid medium by the effect of hydrodynamic forces, thereby forming particle groups in the flow fields. For this reason, flowability is hindered and fluid viscosity increases as well. At this juncture, we should touch upon the significance of particle morphology because hydrodynamic effect gets bigger when the particles have complex morphologies as such in fumed silica [32, 33]. Since fumed silica is composed of branchy particles, hydrodynamic forces drastically increase on these particles, thereby contributing to the shear thickening formation in the suspensions. Furthermore, particle contacts are commonly observed in the mixtures upon shearing at high rates. At these rates, branchy particles lead to interlocking process in the mixtures and provide a booster effect for shear thickening rheology.

It is also important to mention that shear thickening rheology is able to be activated at small excitations without needing high-level loadings. Based on previous works [34, 35], shear thickening onset is visible even at quasi-static conditions, where the stresses are on the order of 10 to 100 Pa. From the rheological measurement results of an STF based on fumed silica and PEG [36], shear thickening onset

is observed at about 10 Pa stresses, which exhibits compatible results with the literature.

## 5.4 STF-Based Vibration Damping in Manufacturing

Vibration damping in manufacturing is quite a new field for STF; however, it possesses a good potential for smart manufacturing applications. Chatter is the main problem based on undesired vibrations in machining operations; however, STF-based solutions date back to only a couple of years. Hence, there is still a big gap to take advantage of shear thickening damping in manufacturing operations.

The first attempt was made by Gürgeç et al. [37] in 2020. In this work, STF was integrated into a cutting tool by drilling a set of STF holes on the top and flank surface of the shank as shown in Fig. 5.9. The holes were covered by a tape after STF filling to prevent from spilling during machining. Modal analysis method was used to determine the damping ratio in the cutting tools. In addition, a set of machining tests was conducted by using different designs of cutting tools and then the surface roughness of the workpieces was measured to understand the role of STF inclusion into the cutting tool. Figure 5.10 shows the experimental setup for the machining and modal analysis system. From the modal analysis results, the damping ratio of the cutting tool increases by filling the holes with STF. However, the damping ratio depends on the hole directions in the cutting tool. The damping ratio is 0.0174% for the conventional tool, whereas it changes to 0.0392% and 0.0225% after STF filling

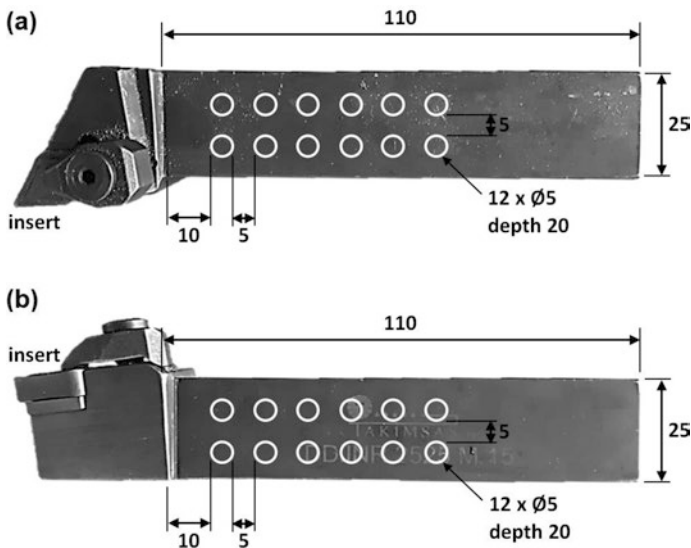
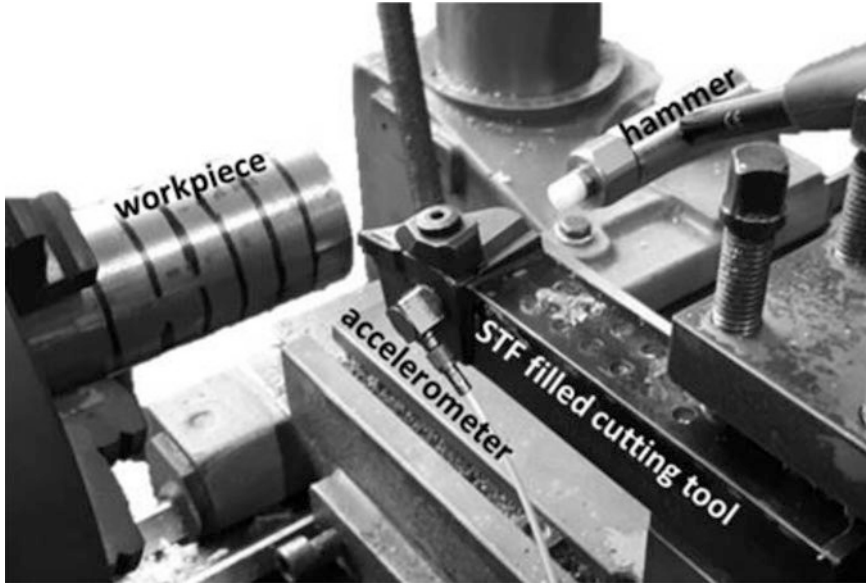


Fig. 5.9 STF holes on the (a) top and (b) flank surface of the shank [37]. Reprinted by permission from Elsevier



**Fig. 5.10** Experimental setup for the machining and modal analysis system [37]. Reprinted by permission from Elsevier

in the top holes and flank holes, respectively. The damping capacity of the cutting tool increases for both STF cases. Figure 5.11 shows the surface topographies for the workpieces machined with different cutting tools. As shown in the images, STF integration leads to a smoother surface finish in comparison to the conventional tool. According to the surface roughness measurements, machining with the conventional tool yields Ra 1.27, while Ra 1.04 and Ra 1.20 are measured for the STF in top and flank holes, respectively. Although STF integration improves both the damping ratio of the cutting tool and the surface finish on the workpiece, hole directions have an importance in the applications.

According to Gürgen et al. [37], chatter-based vibrations act in the feed direction in the machining operation and, therefore, STF in the top holes is excited in the transverse direction, whereas excitation is realized in the longitudinal direction for the STF in the flank holes. It should be noted that particle clusters are able to reach the hole boundaries easily in the top holes compared to the flank holes. Because the peripheral walls in the top holes provide large holding areas for the clustering particles, shear thickening formation grows stronger. In other words, hole boundaries act as rigid bases for the particle clusters, thereby increasing the particle confinement in the suspension. As suggested in previous works [33], particle confinement produces increased shear thickening rheology because confined particle networks are capable of bearing higher stresses without structural breakdown in the particle-contacted microstructure. The mechanism related to this phenomenon is illustrated in Fig. 5.12.



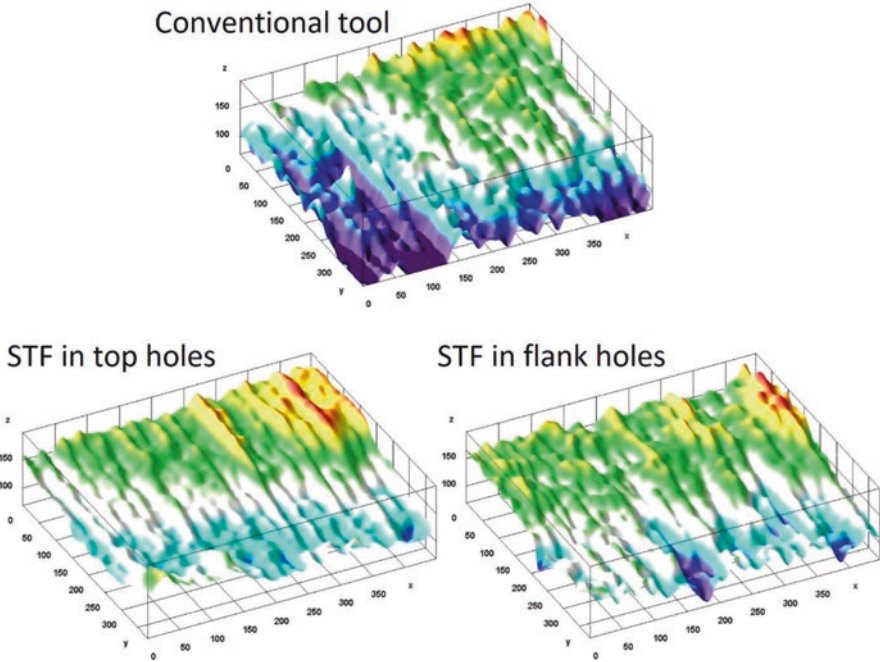


Fig. 5.11 Surface topographies for the workpieces machined with different cutting tools [37]. Reprinted by permission from Elsevier

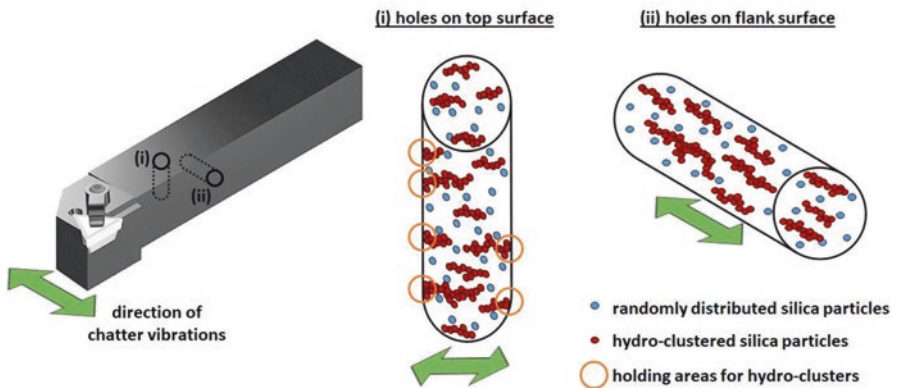
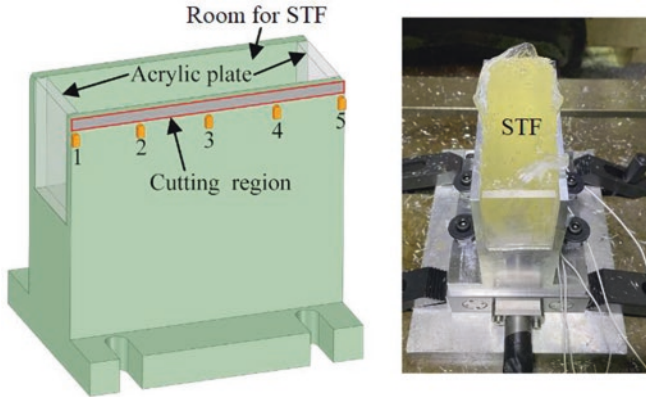


Fig. 5.12 Particle clustering in STF for different cases [37]. Reprinted by permission from Elsevier

Yuan et al. [38] proposed a novel concept regarding the STF-based vibration damping system for the milling of thin-walled parts. Milling is one of the essential operations for shaping the products into final sizes. However, chatter is a big challenge in milling especially for thin-walled parts. In this work, thin-walled parts were



**Fig. 5.13** Experimental setup for milling of thin-walled parts [38]. Reprinted by permission from Elsevier

supported by an STF filler behind the machining face. The outer face was machined by a two-edged carbide tool with 12 mm diameter and  $55^\circ$  helix angle. Feed rate, rotational speed, and cutting depth were 400 mm/min, 5000 rpm, and 0.1 mm, respectively. Five sensors were located at the vibration data collection points as shown in Fig. 5.13. Milling tests were conducted for two cases: (1) without STF and (2) with STF. Figure 5.14 shows the vibration amplitude results from the sensors located at the points 1, 2, and 3. It is clearly seen that vibration amplitudes are suppressed to a great extent by using STF support in the milling operations. At point-1, the peak amplitude is about 30 g without using STF in the machining. The peak amplitude lowers to about 10 g after STF support, which is only one-third of that in the non-STF case. Similar results are observed at points 2 and 3. Another result is the surface roughness on the workpiece after the milling operations. Machined surfaces show more stable surface finish in chatter-free operations. Figure 5.15 shows the surface roughness profiles for different cases. As shown in the charts, milled surfaces include sharp peaks and valleys in the non-STF operations. On the other hand, smoother surfaces are achieved after the milling operations with STF supports. Considering point-5, surface profile varies in a range of  $15\ \mu\text{m}$  without STF support, while the variation range is within only  $2\ \mu\text{m}$  by using STF support in the operation. For the same measurement point, average roughness is  $1.352\ \mu\text{m}$  for the non-STF case and it is lowered to  $0.219\ \mu\text{m}$  by adding STF support in the machining. It is also stated that STF provides a practical approach for chatter suppression in the machining of thin-walled products, which exhibit highly complex vibration characteristics. The product is subjected to different vibrational modes at different locations based on the cutter position. However, STF rheology provides an adaptive behavior for chatter suppression depending on the excitation level. As well as cutter

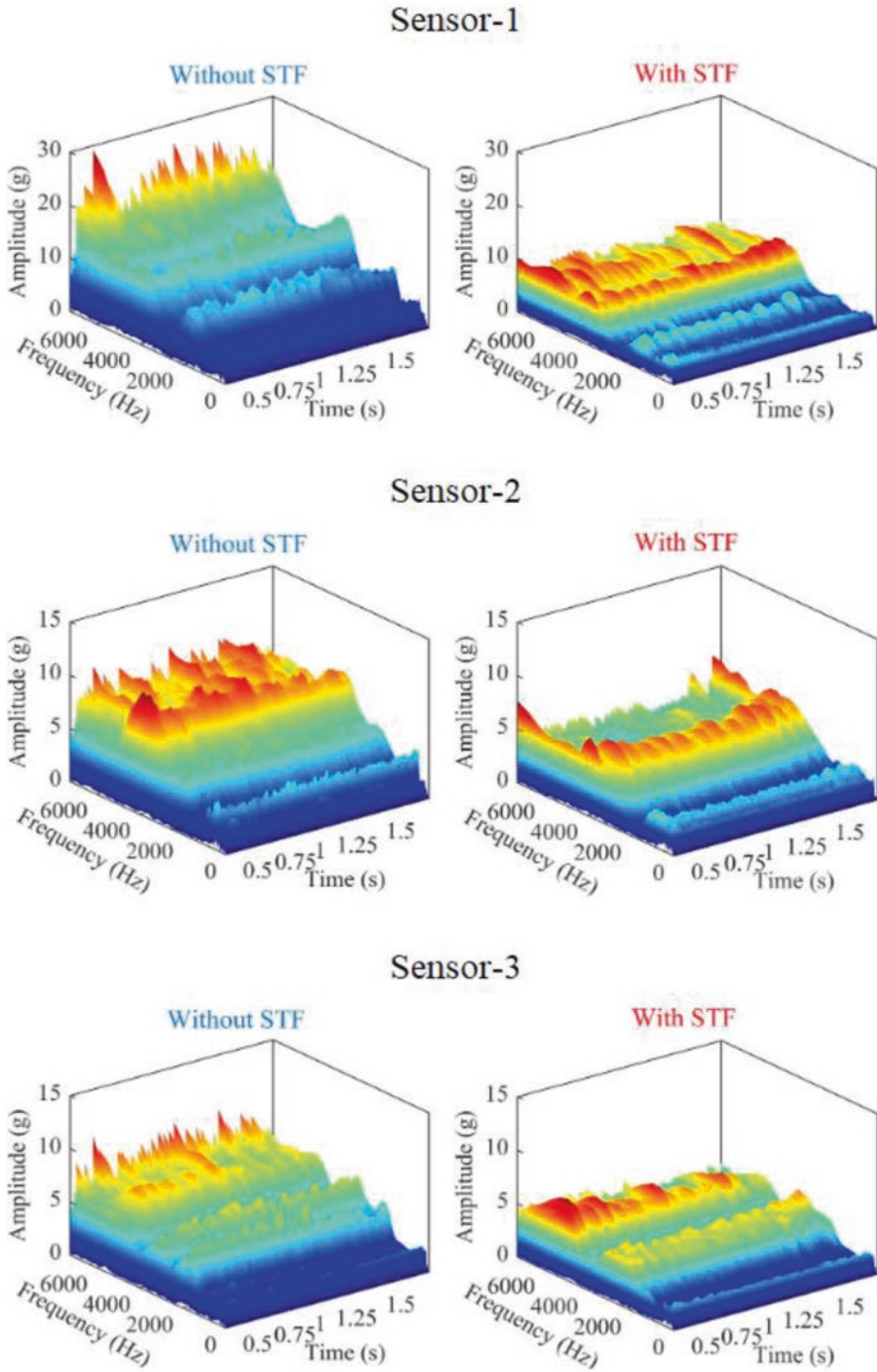


**Fig. 5.14** Vibration amplitude results based on various sensors [38]. Reprinted by permission from Elsevier

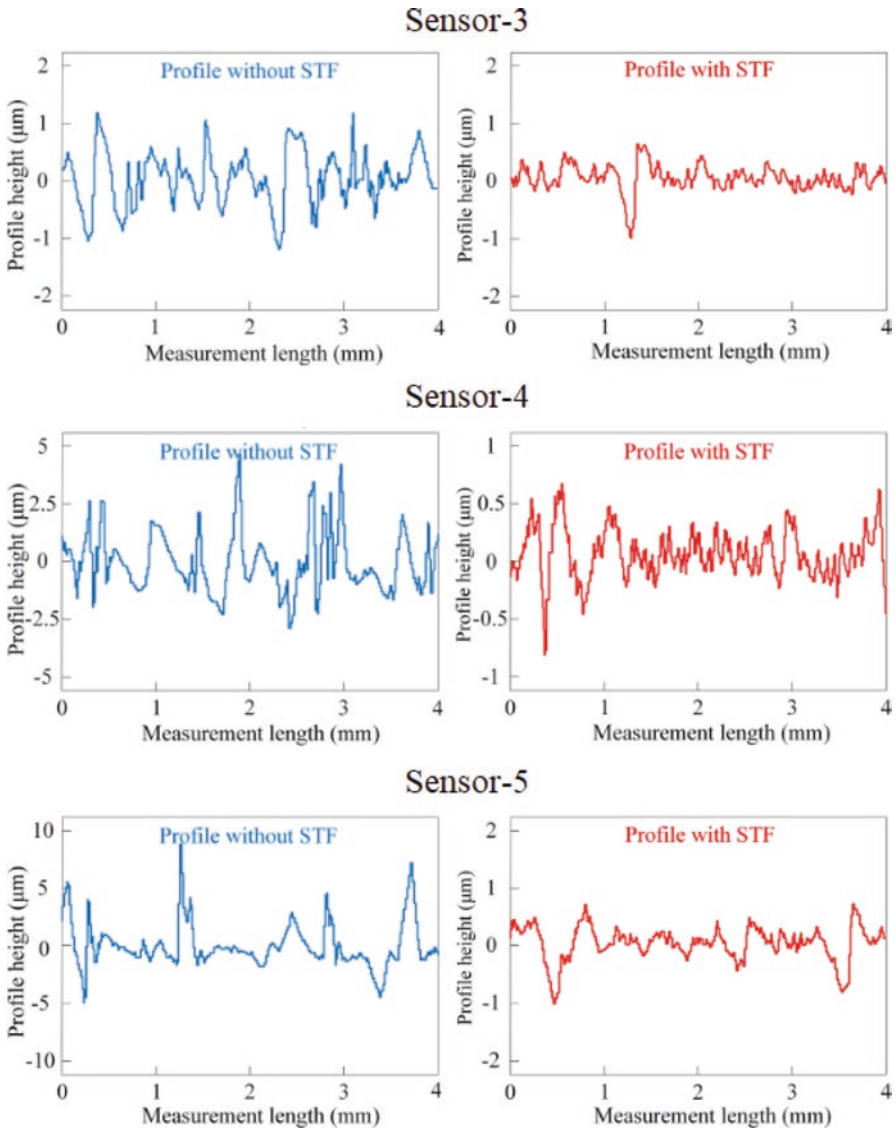


**Fig. 5.15** Surface roughness profiles at different locations [38]. Reprinted by permission from Elsevier

position, cutting force frequency, and cutting force magnitude are determining factors of the vibration characteristics of the machining system. Based on this preliminary work, STF has a promising future in manufacturing applications especially for developing smart adaptive damping operations.

## 5.5 Conclusions

STF is one of the smart materials that shows adaptive rheological behavior for vibration damping systems. For this reason, STF has been adapted to different applications dealing with anti-vibration properties. It is possible to divide the STF-based anti-vibration applications into three groups based on the studies in the literature. A large part of the works is about integrating STF into structural components so that a self-damping behavior is obtained in the structures without requiring additional dampers. Another focus is modifying the conventional dampers by including STF in machinery applications. In general, hydraulic oils are replaced with STF in the conventional damper systems. The damper gets an adaptive damping characteristic by this way. In addition to damper systems, anti-vibration pads are quite common products for vibration attenuation in machinery systems. The latest area for STF-based vibration damping is manufacturing. Undesired vibrations and chatter formation are the most frequent problems in machining operations. STF usage is promising however, STF history is quite short in manufacturing that's why there are only two works in the literature. According to the literature survey conducted in this chapter, STF rheology is suitable for vibration damping systems. STF has a rate sensitive rheology, thereby providing adaptive stiffness and damping properties for anti-vibration applications. Another advantage is that STF is a passive vibration damping material that does not require external stimulation to activate the stiffness and damping behavior. Despite the promising results, there are some drawbacks regarding the STF usage in engineering applications. For example, temperature-dependent rheology in STF restricts the long-term use in damper applications. Nevertheless, STF has a great potential to be adapted to the vibration damping systems after a careful tailoring in the material properties.

## References

1. D.D.L. Chung, Review: Materials for vibration damping. *J. Mater. Sci.* **36**(24), 5733–5737 (2001)
2. X.Q. Zhou, D.Y. Yu, X.Y. Shao, S.Q. Zhang, S. Wang, Research and applications of viscoelastic vibration damping materials: A review. *Compos. Struct.* **136**, 460–480 (2016 Feb)
3. H. Lu, X. Wang, T. Zhang, Z. Cheng, Q. Fang, Design, fabrication, and properties of high damping metal matrix composites—A review. *Materials.* **2**(3), 958–977 (2009 Aug 18)
4. C. Fischer, A. Bennani, V. Michaud, E. Jacquelin, J.A.E. Manson, Structural damping of model sandwich structures using tailored shear thickening fluid compositions. *Smart Mater. Struct.* **19**(3), 035017 (2010 Mar 1)
5. F. Galindo-Rosales, Complex fluids in energy dissipating systems. *Appl. Sci.* **6**(8), 206 (2016 Jul 25)
6. S. Gürgen, F.A.O. Fernandes, R.J.A. de Sousa, M.C. Kuşhan, Development of eco-friendly shock-absorbing Cork composites enhanced by a non-Newtonian fluid. *Appl. Compos. Mater.* **28**(1), 165–179 (2021 Feb)
7. S.S. Shenoy, N.J. Wagner, J.W. Bender, E-FiRST: Electric field responsive shear thickening fluids. *Rheol. Acta* **42**(4), 287–294 (2003 Jul 1)



8. S. Gürgen, A. Sert, Polishing operation of a steel bar in a shear thickening fluid medium. *Compos. Part B Eng.* **175**, 107127 (2019 Oct)
9. S. Gürgen, M.A. Sofuoğlu, Vibration attenuation of sandwich structures filled with shear thickening fluids. *Compos. Part B Eng.* **186**, 107831 (2020 Apr)
10. S.S. Iyer, R. Vedad-Ghavami, H. Lee, M. Liger, H.P. Kavehpour, R.N. Candler, Nonlinear damping for vibration isolation of microsystems using shear thickening fluid. *Appl. Phys. Lett.* **102**(25), 251902 (2013 Jun 24)
11. K.M. Shum, Closed form optimal solution of a tuned liquid column damper for suppressing harmonic vibration of structures. *Eng. Struct.* **31**(1), 84–92 (2009 Jan)
12. C. Fischer, S.A. Braun, P.E. Bourban, V. Michaud, C.J.G. Plummer, J.A.E. Månson, Dynamic properties of sandwich structures with integrated shear-thickening fluids. *Smart Mater. Struct.* **15**(5), 1467–1475 (2006 Oct 1)
13. M. Wei, G. Hu, L. Jin, K. Lin, D. Zou, Forced vibration of a shear thickening fluid sandwich beam. *Smart Mater. Struct.* **25**(5), 055041 (2016 May 1)
14. M. Wei, K. Lin, L. Sun, Shear thickening fluids and their applications. *Mater. Des.* **216**, 110570 (2022 Apr)
15. S. Gürgen, M.A. Sofuoğlu, Experimental investigation on vibration characteristics of shear thickening fluid filled CFRP tubes. *Compos. Struct.* **226**, 111236 (2019 Oct)
16. S. Gürgen, W. Li, M.C. Kuşhan, The rheology of shear thickening fluids with various ceramic particle additives. *Mater. Des.* **104**, 312–319 (2016 Aug)
17. S. Gürgen, An investigation on composite laminates including shear thickening fluid under stab condition. *J. Compos. Mater.* **53**(8), 1111–1122 (2019 Apr)
18. R.C. Neagu, P.E. Bourban, J.A.E. Månson, Micromechanics and damping properties of composites integrating shear thickening fluids. *Compos. Sci. Technol.* **69**(3–4), 515–522 (2009 Mar)
19. S. Gürgen, M.C. Kuşhan, W. Li, Shear thickening fluids in protective applications: A review. *Prog. Polym. Sci.* **75**, 48–72 (2017 Dec)
20. S. Gürgen, Tuning the rheology of Nano-sized silica suspensions with silicon nitride particles. *J Nano Res.* **56**, 63–70 (2019 Feb)
21. S. Gürgen, M.C. Kuşhan, W. Li, The effect of carbide particle additives on rheology of shear thickening fluids. *Korea-Aust Rheol J.* **28**(2), 121–128 (2016 May)
22. Q. Zhao, J. Yuan, H. Jiang, H. Yao, B. Wen, Vibration control of a rotor system by shear thickening fluid dampers. *J. Sound Vib.* **494**, 115883 (2021 Mar)
23. M. Wei, K. Lin, Q. Guo, H. Sun, Characterization and performance analysis of a shear thickening fluid damper. *Meas Control.* **52**(1–2), 72–80 (2019 Jan)
24. K. Lin, H. Liu, M. Wei, A. Zhou, F. Bu, Dynamic performance of shear-thickening fluid damper under long-term cyclic loads. *Smart Mater. Struct.* **28**(2), 025007 (2019 Feb 1)
25. S. Gürgen, M.A. Sofuoğlu, M.C. Kuşhan, Rheological compatibility of multi-phase shear thickening fluid with a phenomenological model. *Smart Mater. Struct.* **28**(3), 035027 (2019 Mar 1)
26. T. Tian, G. Peng, W. Li, J. Ding, M. Nakano, Experimental and modelling study of the effect of temperature on shear thickening fluids. *Korea-Aust Rheol J.* **27**(1), 17–24 (2015 Feb)
27. L. Sun, J. Zhu, M. Wei, C. Zhang, Y. Song, P. Qi, Effect of zirconia nanoparticles on the rheological properties of silica-based shear thickening fluid. *Mater Res Express.* **5**(5), 055705 (2018 May 15)
28. S. Gürgen, M.C. Kuşhan, Rheological properties of shear thickening fluids. *J. Polytech.* **19**(4), 409–414 (2016)
29. S. Gürgen, M.A. Sofuoğlu, M.C. Kuşhan, Rheological modeling of multi-phase shear thickening fluid using an intelligent methodology. *J. Braz. Soc. Mech. Sci. Eng.* **42**(11), 605 (2020 Nov)
30. M. Wei, G. Hu, L. Li, H. Liu, Development and theoretical evaluation of an STF–SF isolator for seismic protection of structures. *Meccanica* **53**(4–5), 841–856 (2018 Mar)
31. S. Gürgen, M.A. Sofuoğlu, Smart polymer integrated cork composites for enhanced vibration damping properties. *Compos. Struct.* **258**, 113200 (2021 Feb)



32. G. Bossis, J.F. Brady, The rheology of Brownian suspensions. *J. Chem. Phys.* **91**(3), 1866–1874 (1989 Aug)
33. S.R. Raghavan, S.A. Khan, Shear-thickening response of Fumed silica suspensions under steady and oscillatory shear. *J. Colloid Interface Sci.* **185**(1), 57–67 (1997 Jan)
34. M.J. Decker, C.J. Halbach, C.H. Nam, N.J. Wagner, E.D. Wetzel, Stab resistance of shear thickening fluid (STF)-treated fabrics. *Compos. Sci. Technol.* **67**(3–4), 565–578 (2007 Mar)
35. B.J. Maranzano, N.J. Wagner, The effects of interparticle interactions and particle size on reversible shear thickening: Hard-sphere colloidal dispersions. *J. Rheol.* **45**(5), 1205–1222 (2001 Sep)
36. S. Gürgen, R.J.A. de Sousa, Rheological and deformation behavior of natural smart suspensions exhibiting shear thickening properties. *Arch Civ Mech Eng.* **20**(4), 110 (2020 Dec)
37. S. Gürgen, M.A. Sofuoğlu, Integration of shear thickening fluid into cutting tools for improved turning operations. *J. Manuf. Process.* **56**, 1146–1154 (2020 Aug)
38. X. Yuan, S. Wang, X. Mao, H. Liu, Z. Liang, Q. Guo, et al., Forced vibration mechanism and suppression method for thin-walled workpiece milling. *Int. J. Mech. Sci.* **230**, 107553 (2022 Sep)